

C.P. No. 160
(15.319)
A.R.C. Technical Report



MINISTRY OF SUPPLY

AERONAUTICAL RESEARCH COUNCIL

CURRENT PAPERS

The Measurement of Position Error at High Speeds and Altitude by Means of a Trailing Static Head

By

K. W. Smith, B.Sc.(Eng.), D.I.C.

LONDON: HER MAJESTY'S STATIONERY OFFICE

1954

Price 3s. 0d. net

June, 1952

ROYAL AIRCRAFT ESTABLISHMENT

The Measurement of Position Error at High Speeds and Altitude
by Means of a Trailing Static Head

by

K.W. Smith, B.Sc. (Eng), D.I.C.

SUMMARY

The static position error of a service wing-tip leading edge pressure head installation has been measured on a Meteor VII by means of a trailing static head, developed especially for use at high speeds.

These tests cover an altitude range from zero to 38,000 ft, and include measurements in 'g' turns. The maximum Mach number reached was 0.84.

For comparative purposes the static error was also measured at ground level by the aneroid method.

The results show that:-

(i) It is possible to develop a trailing static for use to at least $M = 0.84$, and that an accuracy to within ± 0.0025 Mach number can probably be reached.

(ii) At small values of C_L the measured position error agrees approximately with that predicted from the aneroid test results by the Glauert law as far as $M \approx 0.75$. Above this Mach number Weaver's or Charnley's use of the Glauert two-dimensional linearised subsonic flow theory substantially underestimates the measured position error.

(iii) At large C_L 's the Glauert theory appears to break down at comparatively low Mach numbers ($M \approx 0.5$).

(iv) The pressure calibration of the trailing static head agrees with the value found in the wind tunnel to within 0.3% of $\frac{1}{2}\rho v^2$ (at least as far as $M = 0.6$). The tunnel calibration was made by comparing with the pressure on a long static tube, the holes of which were far from the nose.

LIST OF CONTENTS

	Page
1 Introduction	4
2 The problem of position error measurement on current high speed aircraft	4
2.1 Ground level tests	4
2.2 Extrapolation of ground level results to cover other conditions of flight	4
2.3 The desirability of flight results other than at ground level	5
3 Description of equipment used in the Meteor tests	5
3.1 The aircraft and its airspeed installation	5
3.2 The trailing static	5
3.3 Pressure measuring instrumentation	6
4 Calibrations	7
4.1 Calibration of the trailing static head	7
4.11 Tunnel calibrations	7
4.12 Flight calibration	8
4.2 Lag calibration	a
5 Flight tests	9
5.1 Aneroid tests at ground level	9
5.2 Tests with the trailing static	9
5.21 Development of the instrument	9
5.22 Difficulties encountered	9
5.23 Tests in level flight	10
5.24 Tests in dives	10
5.25 Tests in 'g' turns	10
6 Results	11
6.1 Corrections to measurements	11
6.11 Lag	11
6.12 Head calibration	11
6.13 Correction for small height changes	11
6.14 Pressure correction under 'g'	11
6.15 Correction for small speed changes under 'g'	12
6.2 Accuracy	12
6.3 Trailing static results	12
6.4 Position error as a function of lift coefficient and Mach number	13
7 Discussion	13
7.1 Reliability of results	13
7.11 Aneroid results	13
7.12 Trailing static results	13

LIST OF CONTENTS (Contd.)

		Page
7.2	Comparison between trailing static and aneroid results	14
7.3	Comparison between high altitude trailing static results and those predicted by the Glauert law	15
	7.31 Applications of the Glauert law	15
	7.32 Incidence and Mach number & facts on the Mk.VIII head	16
	7.33 Comparison of results	16
8	Future work	17
	8.1 Work with the trailing static	17
	8.2 Possible limitations of the trailing static	18
	8.3 Use of the Meteor as a "calibrated datum"	18
9	Conclusions	18
	References	19
	Notation	20
	Distribution	20

LIST OF ILLUSTRATIONS

	Fig.
Details of aircraft and airspeed installation	1
Details of high speed trailing static head	2
Static pressure error as measured by trailing static head in unaccelerated flight	3
Static pressure error as measured by trailing static head in 'g' turns	4
Comparison between static pressure errors as measured by trailing static and by aneroid method at ground level	5
Static pressure error coefficient as a function of Mach numbers for various altitudes in unaccelerated flight	6
Static pressure error coefficient as a function of lift coefficient	7
Comparison between flight values of static error and those predicted from ground level aneroid results by Weaver's method	8
Comparison between flight values of static error and those predicted by equation of the form	9
$\Delta C_P = \frac{\Delta C_{P_0}}{\sqrt{1 - M^2}} - KC_L^2$	
Comparison between flight values of static error and Mach number error at 30,000 ft in unaccelerated flight with those predicted by extrapolation of ground level results	10
Relation between static pressure error and corresponding Mach number error in subsonic flow	11
The trailing static head being towed behind Meteor	12

1 Introduction

The complete measurement of the position error of present day high speed aircraft has so far proved a difficult problem. Limited results have been obtained fairly easily at ground level, but these have been insufficient to establish curves covering the whole flight range of speed, altitude and normal acceleration.

Theoretical methods for extrapolating the limited ground level results to cover the whole flight range have been developed, but these methods are expected to break down at Mach numbers above the critical, while little evidence has so far been obtained to check their reliability at sub-critical speeds.

Thus, in order to provide experimental data on position error both at high speeds and high altitudes, several flight techniques have been tried out during the last few years, both in America and this country. One of these techniques consists of towing a trailing static head, developed especially for use at high speeds.

It is the first results obtained by means of this instrument that are presented in this note. They are thought to be interesting as they appear to possess sufficient accuracy to indicate clearly the separate effects of Mach number and lift coefficient on the static position error of the particular installation that has been tested.

2 The problem of position error measurement on current high speed aircraft

2.1 Ground level tests

Considering only the static error (the pitot error is only likely to be appreciable near the stall, and in cases where a shock wave is formed ahead of the pitot tube) it has been relatively easy to determine this at ground level by the 'aneroid' method.

This method, however, limits the results obtained to the maximum safe level speed near the ground. In many cases this excludes the most interesting region of flight, namely the Mach number range between the first formation of shock waves and the maximum obtainable by diving.

Also, the results of an aneroid test cannot be used directly to give the position error under conditions of flight corresponding to a combination of high Mach number and high lift coefficient.

2.2 Extrapolation of ground level results to cover other conditions of flight

Theoretical methods^{1,2} have been devised during the last few years for extrapolating the measured ground level position error curve to cover conditions giving rise to different combinations of Mach number and lift coefficient. These methods, therefore, allow the error to be estimated at high altitude and under 'g', and although each method of analysis expresses the effect of compressibility in a general form, it suggests that the Glauert-Prandtl law is used until experimental evidence becomes available. However, it is known that this law has a number of theoretical limitations, the most important one being that it cannot be applied to flow in which shock waves are present.

2.3 The desirability of flight results other than at ground level

Due to the limitations of the Glauert law it is very desirable to obtain experimental data on position error, measured over a wide range of altitude and 'g', as well as at high Mach numbers, above the critical value. Although the results at high Mach number are of prime interest, those at medium Mach numbers are also required, in order to check the accuracy of the position error predicted from the simple ground level tests.

3 Description of equipment used in the Meteor tests

3.1 The aircraft and its airspeed installation

The aircraft used was a standard Meteor VII. A general arrangement of the aircraft is presented in Fig.1(a). Most of the tests were made with no external fuel tanks fitted. However, a limited amount of work was done with the two underwing tanks in position.

All the position error measurements were made on the service airspeed installation, shown in Fig.1(b). It consisted of a Mk.VIII pressure-head, mounted on a boom, which projected 41% of the local wing chord ahead of the wing leading edge, at a spanwise location near to the port wing tip. The thickness/chord ratio of the wing at this spanwise location was 10%.

3.2 The trailing static

The trailing static head itself is shown in Fig.2, together with relevant numerical data.

The head was constructed with a mainplane and tail surfaces, the latter being set so that the mainplane was trimmed to give a downward lifting force. This downward force was required to ensure that the head trailed clear of the aircraft wake. Towing was by means of a hollow cable, the line of which passed through the centre of gravity of the head; thus the lift coefficient of the mainplane would be independent of speed, at least below the critical Mach number.

The pressure recorded by the trailing static head was transmitted to the parent aircraft through a hollow cable, the free length of which was between 78 and 90 ft. This cable was also required to transmit the loads arising on the head in flight.

Two types of cable piping were used during the tests. The first consisted of a rubber covered Bowden tube, which was braided externally with steel wire, in order to provide the necessary tensile strength. Its outside diameter was 0.28 ins, and the breaking load was 525 lbs. The second was of molybdenum steel, heat treated to ensure adequate flexibility. It was adopted after successful flight tests as being superior to the first type; its tensile strength was greater (825 lbs), while the external diameter was less (0.137 ins). Both pipes had an internal diameter of 0.10 ins.

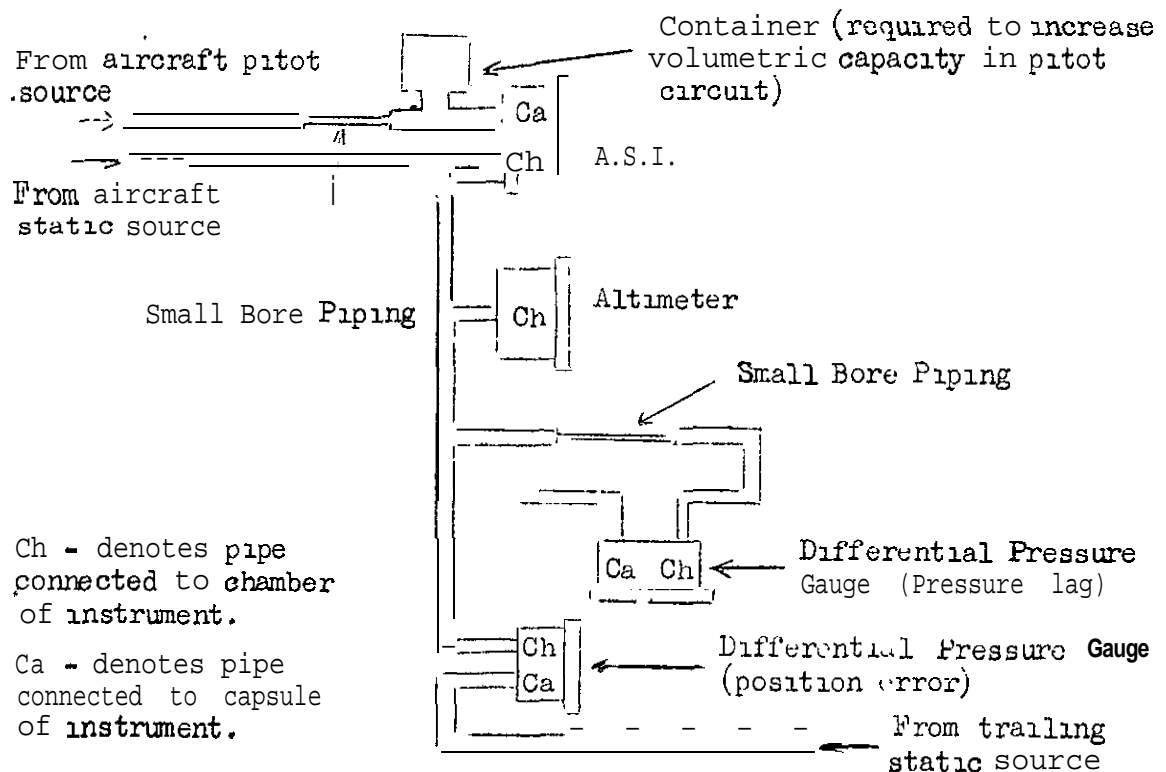
The trailing static head was lowered from the aircraft by means of an electrically operated winch of overall dimensions 12 ins x 11 ins x 7 ins (excluding the motor). When raised, the trailing head was held in a crutch on the underside of the Meteor fuselage (see Fig.1(a)). The pressure in the cable piping was transmitted through a seal in the winch shaft to a pressure instrument in the auto-observer.

The trailing static is shown being towed behind the Meteor in Fig.12.

3.3 Pressure measuring instrumentation

The indicated values of airspeed, pressure altitude and Mach number were measured from an A.S.I. and altimeter connected to the pitot and static sources from the wing-tip pressure head. The static position error of the wing-tip head was measured directly by a differential pressure gauge (range -5 to +5 ins water) connected between the aircraft static and trailing static pressure sources.

As some of the flight tests involved dives, compensation for pressure lag in the various pipelines was found to be necessary. The apparatus used for this, together with all the pressure instrument connections, is shown in the sketch below:-



The detailed procedure for pressure lag compensation during dives will be described in para. 4.2, but at this stage the purpose of the various components can be outlined as follows:-

(i) The container and length of small bore piping in the pitot line were inserted in order to approximately balance the steady lags in the pitot and static lines of the aircraft pressure head circuit.

(ii) No adjustment to the trailing static line was necessary, as it possessed approximately the same steady lag characteristic as that of the aircraft static.

(iii) The pressure drop along a length of small-bore piping, fed from the aircraft static source, was measured with a differential pressure gauge, in order to obtain knowledge of the actual pressure lag along a line of known characteristics during any dive.

The four pressure instruments, together with a remote indicating Barnes type 'B' accelerometer, were mounted in an auto-observer. The instruments were photographed with a Vinten cine camera.

4 Calibrations

4.1 Calibration of the trailing static head

4.11 Tunnel calibrations

Each of the five trailing static heads used in flight were subjected to a calibration in the R.A.E. 5 ft open jet tunnel.

With the centre of gravity exactly at the free suspension point, the curve of lift against tail-setting angle was established. The pressure measured by the static head was also recorded over a range of tail-setting angles.

Most of these tests were made at a wind speed of 20 ft/sec, but a few were done at 180 ft/sec. No significantly different results were obtained at the higher speed.

Due to manufacturing errors, the lift/tail-setting curve for one model was found to be non-repeatable on another one. The discrepancy between models (the maximum was ± 0.125 in C_L for a given geometrical tail-setting) was sufficient to warrant individual calibrations.

The static pressure in the tunnel, at the position occupied by the trailing static head, was later calibrated with the R.A.E. standard pressure head.

At the time of the tunnel calibration tests the R.A.E. head was believed to indicate a static pressure $0.0125 \times \frac{1}{2}\rho V^2$ below the true value. On this assumption the trailing static head calibration was

$$\frac{P_T - P_s}{\frac{1}{2}\rho V^2} = - 0.008 \quad (1a)$$

where P_T = pressure indicated by trailing static head

P_s = free stream static pressure.

Equation 1a was found to hold within ± 0.002 for each head tested, over the CL range of zero to -0.3.

Later, when equation 1a was compared with the results of flight calibration, it was suspected that the R.A.E. static head calibration was unreliable. The R.A.E. head was recalibrated (against a head on which the static holes were very far behind the nose*) and was found to really indicate a pressure $0.0025 \times \frac{1}{2}\rho V^2$ below true static. Thus, equation 1a should be modified to read

$$\frac{P_T - P_s}{\frac{1}{2}\rho V^2} = + 0.002 \quad (1b)$$

*The head was 0.5 inches diameter and had an elliptic nose of length/diameter ratio 3. The static holes were 12.5 diameter behind the nose and 32 diameters ahead of a $\frac{1}{4}$ inch high shoulder. The calculated pressure on the holes was $0.0007 \times \frac{1}{2}\rho V^2$ higher than true static.

4.12 Flight calibration

A calibration of the trailing static head was found in flight by comparing the ground level position error measurements as found by the 'aneroid' and trailing static methods.

Reference to Figs 5a and 5b shows that for the flights without under wing tanks

$$\frac{\Delta P_S - \Delta P_T}{\frac{1}{2}\rho v^2} = \frac{P_T - P_S}{\frac{1}{2}\rho v^2} = + 0.005 \quad (1c)$$

while in the case with tanks

$$\frac{\Delta P_S - \Delta P_T}{\frac{1}{2}\rho v^2} = \frac{P_T - P_S}{\frac{1}{2}\rho v^2} = + 0.0075 \quad (1d)$$

A mean value of $\frac{P_T - P_S}{\frac{1}{2}\rho v^2}$ equal to +0.005 has been used when evaluating all position errors from the trailing static results.

4.2 Lag calibration

A report is at present being written concerning both the theory and practice of pressure lag measurement in pipes, and for this reason a detailed description of the compensation technique used will not be given here. Nevertheless, as the accuracy of the position error measurements at the high Mach numbers depended on a reliable lag correction, an outline of the method is thought to be desirable.

The object of the ground tests was to measure the relative lags in the various sections of the pressure system, including that across the small-bore piping fed from the aircraft static source, during simulated steady descents. A steady descent was reproduced by partially evacuating the particular system being tested, and then allowing air to re-enter from the outside atmosphere. The incoming air was controlled by a hand-operated valve at the "input" end (e.g. at the static head) in such a manner that a very nearly steady descent was provided. The pressure drop along each section was then measured directly with a differential pressure gauge.

By recording the actual pressure drop across the static-fed small-bore piping during a particular flight dive, it would thus be possible to estimate, by simple proportion, the actual steady lag in any part of the pressure system during that same dive.

The ground tests were done at various rates of simulated descent, going as high as the maximum that was likely to be met in flight. After some slight modifications, the lags in all parts of the system were found to be linear functions of the rate of descent. The values obtained are given below:-

/Table

Stations between which Pressure Drop was Measured	Pressure Drop for 100 ft/sec Rate of Descent (lb/ft ²)	Equivalent error at M = 0.3 and 30,000 ft	
		Pressure Coefficient	Mach number
Each end of the small-bore piping fed by the aircraft static (i.e. across the lag differential gauge)	4.78	-	-
Aircraft static head and auto-observer instruments (aircraft static line)	5.51	-0.0195	+0.0088
Trailing static head and auto-observer differential gauge (trailing static line)	6.19	-0.0219	+0.0098
Aircraft pitot head and auto-observer A.S.I. (pitot line)	3.69	+0.0131	-0.0039

5 Flight tests

The relevant pressure lines were tested for leaks before each flight, and wherever possible, after each flight. Results from flights in which a leak was suspected were disregarded.

5.1 Aneroid tests at ground level

Six flights were made; two with the external fuel tanks fitted, and four without them. The norm.1 auto-observer altimeter was replaced by a hand-picked one, selected for its low value of hysteresis lag. Runs were made at between 40 and 150 feet above the runway.

5.2 Tests with the trailing static

5.21 Development of the instrument

A considerable proportion of the ninety flights so far made with the trailing static were devoted to the development of the instrument itself. Prior to fitting the installation in a Meteor it was flown from a Lancaster. These first tests were designed to reveal my low speed difficulties, and resulted in a number of minor modifications to both the trailing head and the crutch.

5.22 Difficulties encountered

A considerable number of troubles, both mechanical and aerodynamic, were encountered during the tests on the Meteor. All these difficulties were eventually overcome, and are briefly described below -

(i) The first type of towing pipe used (braided) developed leaks after a number of flights and seemed to have a fairly short life. Similar trouble was not encountered with the plain metal pipe.

(ii) A failure of the winch was experienced when the model was trailing. It was due to a breakage in the flexible drive between the motor and winch. The drive was later increased in size

(iii) Two models were lost by cable failure when in the crutched position. Model loads could have been considerably reduced by decreasing the local incidence of the crutch, but this was not done. Instead, an A.S.I. limitation of 300 knots was imposed when the model was crutched, and no further cable failure was experienced.

(iv) The first four static heads which were towed, initially flew asymmetrically behind the Meteor. The asymmetry increased with indicated airspeed and was thought to be due to manufacturing errors in the model. The effect was virtually eliminated by fitting ailerons (Fig.2) and trimming them by trial and error.

The last two heads, which incidentally possessed an unproved surface finish, required no such lateral trimming.

(v) When the plain steel towing Pipe was first used an undamped fore and aft oscillation of the towing system developed at about $M = 0.65$. This instability was believed to be due to the pipe having unusual drag characteristics (namely a drag which decreased with increasing speed over a particular Mach number range). These drag characteristics resulted in negative damping of the fore and aft motion. Stability was achieved by fitting small plates to the fin of the model (Fig.2), thereby increasing the model drag and providing a positive damping contribution.

5.23 Tests in level flight

The heads were trimmed to give downward lift in all cases, C_L varying between -0.2 and -0.32. The length of trailing pipe was between 76 and 90 feet.

Initially, the level tests were made at a series of steady speeds, but when it was found that identical results were obtained by slowly and continuously increasing the speed (at about 1-2 knots per second), the latter technique was adopted.

Tests were made at a series of constant indicated altitudes between ground level and 30,000 ft.

A test was also made to determine the effect of towlength on the measured position error pressure difference. This was done at low altitude and 200 knots I.A.S. No significant variation in recorded pressure was noticed until the towlength was reduced to about 40 feet, so that it was apparent that no aircraft disturbances were present at the trailing head when at full towlength.

All tests were made without wing tanks fitting, except at sea level, where they were also done with the tanks on.

5.24 Tests in dives

These were done at 20,000 and 30,000 indicated feet. No tanks were fitted. A number of dives were made, each dive being started several thousand feet above the test height, the pilot aiming to reach a steady Mach number as the correct height was passed. Auto-observer records were taken from 1000 ft above the test altitude to 1000 ft below it. Dives with an unsteady descent were discounted.

The maximum Mach number reached ($M = 0.843$) represents the practical limit for this particular aircraft, the limit being imposed by wing-drooping.

5.25 Tests in 'g' turns

These were done at 30,000 indicated feet, without wing tanks.

The effect of 'g' on position error was investigated in steady turns, rather than in pull-outs, because of the uncertainty of lag corrections in an unsteady descent.

The tests were made at a series of indicated airspeeds from 200 to 295 knots, the 'g' being increased in small increments at all speeds. Auto-observer records were taken only when a steady speed and 'g' were attained. At the higher speeds, where diving was necessary at high 'g', the pilot aimed to reach steady conditions at the test altitude.

Most of the work was done in left hand turns (the pressure head was on the port wing-tip), but a few runs, at 200 knots, were made in right hand turns. As can be seen from Fig. 4, no significant effect appears to arise as a result of asymmetry.

6 Results

6.1 Corrections to measurements

6.11 Lag

In accordance with the technique described in para. 4.2, all lag corrections are given by

$$p_o = p_i - R_\ell \cdot \Delta p_\ell \quad (2)$$

where p_i = pressure at pressure head

p_o = pressure at instrument

Δp_ℓ = measured pressure drop along the small-bore piping fed from the aircraft static source

$R_\ell = \frac{\text{lag in particular part of system}}{\text{lag in small-bore piping}}$ (found from ground calibration)

6.12 Head calibration

Tunnel and flight tests suggest that the trailing static head reads a pressure from 0.2% to 0.7% of $\frac{1}{2}\rho V^2$ higher than true static, and a mean value of 0.5% (see equation 1) has been adopted in estimating true position errors from the apparent values measured by the differential pressure gauge between the aircraft and trailing static heads. The same calibration factor has been used for all Mach numbers.

6.13 Correction for small height changes

In practice the dives were not all steadied at exactly the correct test altitude, variations of 1500 ft being encountered. Now at high speeds it can be seen that the position error depends more on Mach number than lift coefficient (Fig. 7). Thus the dive results of Fig. 3 have been corrected to the test altitude at constant Mach number; the pressure error has been multiplied by the factor $\left[\frac{\text{I.A.S. at required altitude}^2}{\text{I.A.S. at actual altitude}^2} \right]$, and the indicated airspeed has been adjusted to keep the Mach number constant.

6.14 Pressure correction under 'g'

Under 'g' the atmospheric pressure difference between the trailing static head and the instruments is $\rho g \Delta h_t$, while the pressure drop along the trailing pipe is $n \rho g \Delta h_t$.

Hence

$$P_o = P_i + (n-1)\rho g \Delta h_t \quad (3)$$

Where p_i = pressure at trailing static head

P_o = pressure at instrument

n = total normal acceleration factor

ρ = free stream density corresponding to aircraft (or trailing static) height

g = acceleration due to gravity

Δh_t = vertical height of instrument above trailing static

Over the speed range of the 'g' tests Δh_t was about 30 ft, so that the correction of equation 3 was just appreciable.

6.15 Correction for small speed changes under 'g'

It proved impossible to make all the 'g' tests at exactly the nominal A.S. I. readings required, variations of about ± 7 knots being tolerated. Now the position error results under 'g' are plotted in Fig.4 as $[(APT) - (\Delta P_T)_{n=1}]$ against n (APT is the apparent static position error and n is the total 'g'). In determining the quantity inside the bracket, $(\Delta P_T)_{n=1}$ was taken corresponding to the actual A.S.I. reading rather than to the nominal value.

6.2 Accuracy

Apart from the possibility of systematic errors (discussed in para 7.1) it appears from the scatter of points in Fig.7 that, at high Mach numbers, an accuracy of about ± 0.005 in pressure coefficient (or ± 0.0025 in Mach number) can be expected by using the trailing static. These results were obtained by using the faired curves through individual flight points.

6.3 Trailing static results

The measured pressure error results are given in Fig.3 (unaccelerated flight) and Fig.4 ('g' turns). All corrections have been applied except that for the trailing static head calibration. The results of Figs. 3 and 4 are for the Meteor without underwing tanks. Ground level results for the case with tanks are presented in Fig.5(b). These are only for ground level, and are shown chiefly for comparison with the corresponding aneroid results.

The results under 'g' show a fair amount of scatter at the higher speeds. It is felt that this could be reduced considerably. Pilots experienced difficulty in maintaining thoroughly steady conditions during the 'g' tests, and their performance would have undoubtedly improved with more than the limited practice they were able to obtain.

The actual "static pressure" errors have been converted to a non-dimensional coefficient form, and presented as such in Figs 6 and 7. This method has been adopted, rather than that in which position error is presented as a correction to altimeter and A.S.I. readings, as it is the more useful one when it is desired to determine the effect of M and C_L on position error.

6.4 Position error as a function of lift coefficient and Mach number

The static pressure error coefficient is plotted as a function of C_L for various values of Mach number in Fig. 7. The curves have been obtained from the results of Fig. 6 (unaccelerated flight) and Fig. 4 ('g' turns).

The lift coefficient has been obtained from the following equation, which is accurate to within 0.1%:-

$$C_L = \frac{n\bar{w}}{\frac{\gamma}{2} P_S M^2 \left[1 - \Delta C_P \cdot \frac{\gamma}{2} M^2 \right]} \quad (4)$$

where \bar{w} = wing loading

P_S = static pressure corresponding to indicated height

M = true Mach number.

A mean wing loading of 38.0 lb/ft² has been assumed for use in equation (4), the error involved being not more than ±2%.

Although the curves of ΔC_P against C_L are themselves obtained by cross-plotting the paired curves of position error at various altitudes and under different values of 'g', the curves plotted against C_L contain points themselves. The practice of marking experimental points on cross-plotted curves is not usually justified, but in this particular case it was thought to be desirable in observing the scatter between results at various altitudes, and also in ascertaining the degree of correlation between results in unaccelerated flight and those under 'g'.

6.4 Aneroid results

These are plotted in Fig. 5(a) (no external tanks) and in Fig. 5(b) (with external tanks); corresponding ground level results obtained with the trailing static are presented for comparison.

7 Discussion

7.1 Reliability of results

7.11 Aneroid results

Normally the aneroid method should provide a reasonably accurate means of measuring the true static pressure error. There is however, one source of inaccuracy that should be investigated, namely the presence of ground effect. This has been done and found to be negligible. The theoretical calculations assuming the lift to be replaced by a bound vortex and two trailing vortices have shown that the magnitude of this error is less than can be measured by existing instrumentation. Further confirmation was obtained when no correlation appeared to exist between the measured position error and the particular height of the aircraft above the ground.

7.12 Trailing static results

Three possible sources of inaccuracy have been studied:-

(1) Disturbances from the aircraft reaching the trailing static. The measurements on variable tow length have shown that this effect is small

for a cable length of 78 ft at low mach numbers, even at high C_L . Further confirmation was obtained when calculations assuming the lift to be replaced by a bound vortex and two trailing vortices showed that the pressure error at the position of the trailing static head was negligible in incompressible flow. As yet there is no experimental evidence to show that no disturbance reaches the trailing static at high Mach number. Although pressure disturbances decay less rapidly with increasing Mach number, the rate of decay would have to be much reduced if the calculated static pressure error was to be significant at the trailing static head. Some experimental data could be obtained in flight by finding the effect of towlength on pressure measurements.

(ii) Variation in pressure calibration of the trailing static head. In evaluating true static position errors the trailing static head has been assumed to measure a pressure equal to $0.005 \times \frac{1}{2}\rho V^2$ higher than true static. This calibration has only been confirmed experimentally as far as $M = 0.62$ (i.e. the maximum speed reached by the trailing static at ground level), although there is evidence to show that it will hold at least as far as the maximum Mach number reached by the Meteor. Tunnel results⁴ indicate that the pressure calibration due to the static tube alone will not alter until $M = 0.85$. In addition some American wing-flow data shows that blockage from the fuselage of the trailing static head will not change until the critical Mach number of the fuselage is reached. This will be at about $M = 0.9$.

(iii) Lag correction during dives. The correction has been applied assuming that the pressure input is the same at each of the three sources (aircraft static, aircraft pitot and trailing static). This is not strictly accurate, but the error involved by a finite rate of change of airspeed and position error has been calculated to be negligible in the tests so far made.

It must be emphasized that the lag correction during the steepest dives is of the same order as the position error being measured so that considerable accuracy is desirable when estimating the correction. A flight check of this could be made by obtaining additional position error results at reduced engine power, and comparing them with results at higher power.

7.2 Comparison between trailing static and aneroid results

Fig. 5 shows that the true static position error at ground level P_S is given, within the accuracy of measurement, by:-

$$\Delta P_T + 0.005 \times \frac{1}{2}\rho V^2 \text{ for the aircraft with wing tanks}$$

$$\Delta P_T + 0.0075 \times \frac{1}{2}\rho V^2 \text{ for the aircraft without wing tanks.}$$

This establishes the flight calibrations of the trailing static head which are given by equations 1(c) and 1(d). The discrepancy of 0.2% between the two flight calibrations cannot be accounted for, as it is somewhat larger than the scatter of the trailing static or aneroid results.

A slight discrepancy between tunnel and flight calibrations of the trailing static head also exists. If a mean calibration given by equation 1(c) is assumed, then tunnel and flight results, given by equations 1(b), 1(c) and 1(d) agree to within $\pm 0.3\%$ of this value.

The flight calibration of the trailing static head is the first absolute calibration of a static head that has been obtained since the

tests on the N.P.L. whirling arm⁷ in 1912. The flight tests have been made at speeds considerably higher than those on the whirling arm (the latter being 60 ft/sec).

7.3 Comparison between high altitude trailing static results and those predicted by the Glauert law

7.3¹ Applications of the Glauert law

A number of methods have been developed for extrapolating ground level static position error measurements to cover other conditions of flight. Each of these methods is such that the effect of compressibility can be expressed in a general form although, as more theoretical and experimental evidence is lacking, it has been suggested that the Glauert law is used.

As the applications of the law differ somewhat in each method it would probably be useful to state the basic law at this stage:-

"The two-dimensional compressible flow around an aerofoil at Mach number M is found by solving the incompressible flow around an equivalent section whose ordinates parallel to the free stream are unaltered, but whose ordination normal to this direction are multiplied by the factor

$$\frac{1}{\sqrt{1-M^2}}."$$

This means that the equivalent section has a thickness and incidence $\frac{1}{\sqrt{1-M^2}}$ times the corresponding values for the actual section in compressible flow.

The Glauert law is limited to inviscid flow which is subsonic and shock free. It is also linearised so that, strictly speaking, it is only applicable to very thin sections.

The applications of the law to static position error are themselves approximate, apart from the limitations of Glauert's theory. It is important to state that no claims to their accuracy have been made. They were intended only to be sufficiently reliable for practical purposes, while remaining simple to apply.

Weaver's¹ method states that the static pressure error is related to the parameters lift coefficient and Mach number by the equation

$$\Delta C_P \sqrt{1-M^2} = f [C_L \sqrt{1-M^2}] \quad (5)$$

where the function f is determined experimentally from the ground level aneroid test for any particular system.

Charnley's² application states, apart from some unimportant approximations, that if at ground level the static pressure error coefficient is $(\Delta C_P)_{h=0}$, and the Mach number is M_0 , then at a different altitude at the same lift coefficient and at a Mach number M_h , the static pressure error coefficient lies between the limits given by

$$(\Delta C_P)_{h=0} \quad \text{and} \quad (\Delta C_P)_{h=0} \frac{\sqrt{1-M_0^2}}{\sqrt{1-M_h^2}}$$

A third application has been devised by solving the two-dimensional potential flow around a section similar to that of the Meteor wing, using the Glauert law to find the equivalent incompressible section. The pressure error at a point on the chord line corresponding to the aircraft static head has been computed, and was found to be of the form

$$\Delta C_D = \frac{\Delta C_{P_0}}{\sqrt{1-M^2}} - KC_L^2 \quad (6)$$

where ΔC_{P_0} and K are constants.

It should be emphasized that equation (6) is only likely to apply to an airspeed installation mounted on the chordline of a wing section with small camber. Equation (6) is similar to that derived by Cameron³, except that his second term is in C_L rather than in C_L^2 .

7.32 Incidence and Mach number effects on the Mk.VIII head

The Glauert law and its application do not take into account any static position error that is incurred by the aircraft static head not reading the local static pressure. The difference between local static and recorded pressures will be influenced by Mach number and local incidence of the head. Tunnel tests⁴ show that at zero incidence the rise in pressure recorded by the standard leading edge static head (Mk.VIII A) is less than 0.5% of $\frac{1}{2}\rho V^2$ between low speed and $M = 0.85$, but from Refs. 4 and 5 it would seem that there is some doubt regarding the low speed calibration of the head. Nevertheless, it would probably read between 0.5% and 2% of $\frac{1}{2}\rho V^2$ above the local static pressure.

Tunnel tests⁵ show that at 10° incidence the pressure recorded by the Mk.VIII head is lowered by about 2% of $\frac{1}{2}\rho V^2$ for all Mach numbers up to 0.84.

It may be concluded that Mach number and incidence effects on the Mk.VIII head itself will be sufficient to modify slightly the total static position error, but they are not likely to alter it fundamentally.

7.33 Comparison of results

The experimental variation of static position error is shown in Fig. 7. From this it can be seen that agreement between tests in unaccelerated flight and 'g' turns is generally good. This fact suggests that the effects of pitching velocity and aero-elastic distortion upon position error are small in the case of the Meteor. The latter effect is not likely to be appreciable for a low aspect ratio unswept wing, whereas it might be considerably larger for a high aspect ratio swept wing. For this reason it would be unwise, at present, to generalise about the effect of distortion on position error.

The curves of ΔC_D against C_L for various values of M are compared with those estimated by Weaver's method in Fig. 8. Agreement is fairly good for small C_L values up to about $M = 0.75$, but above this Mach number the actual blockage offered by the wing increases considerably above the value predicted by extrapolating the anemometer results. At larger C_L 's the measured blockage increases above that predicted at considerably lower values of Mach number; in fact the discrepancy appears to commence at about $M = 0.5$.

The discrepancy at high C_L ($C_L > 0.65$) between the measured and estimated curves that occurs at low Mach numbers can be attributed to

scatter in the experimental results (see Fig.7). These results were obtained at low A.S.I. readings where a small pressure represents a comparatively large pressure coefficient.

In Fig.9 a comparison is made between the measured ΔC_p and that estimated from equation 6, where the constants ΔC_{p0} and K have been found by fitting the best curve to the experimental results at low speed ($M < 0.4$). The same general comparison is obtained as was found in Fig.8, and in addition it can be seen that the low speed curve of ΔC_p against C_L is very nearly parabolic, as predicted by equation 6.

It appears that the rise in pressure blockage at the aircraft static head is associated with the formation of shock waves on the wing. At Mach numbers higher than the value required for shock wave formation the wing pressure distribution will differ from that predicted by the Glauert law and this could affect the pressure at some point ahead of the wing.

Also it is known that, on a given aircraft, shock waves are formed at progressively lower Mach numbers as the lift coefficient is increased.

Fig.10 compares measured and estimated static pressure error coefficient and Mach number error at 30,000 ft in unaccelerated flight. The Mach number error has been estimated from the corresponding static pressure error coefficient from the equation

$$\frac{\Delta M}{\Delta C_p} = -\frac{11}{2} \left[1 + \frac{\gamma-1}{2} M^2 \right] \quad (7)$$

This equation, which has been obtained in a somewhat different form in Ref.6, is obtained by differentiation of the equation relating static and total head pressures to Mach number. It therefore neglects second order terms and is only true for very small values of ΔM . The values of ΔM in Fig.10(b) have been estimated from equation 7, M being replaced by the mean of the true and indicated Mach numbers $\left(\frac{M_{true} + M_{indicated}}{2} \right)$, given by equation 7, is plotted against M in Fig.11.

From Fig.10 it appears that as far as $M = 0.75$ the measured error lies below the curve estimated by Weaver and somewhere between the alternative curves of Charnley. Above this Mach number the static pressure error coefficient and Mach number correction increase rapidly in the positive sense, exceeding considerably the estimated values. At an indicated Mach number of 0.80, the true Mach number is about 0.018 higher than that predicted by Weaver's method.

8 Future work

8.1 Work with the trailing static

Some results have been obtained with underwing tanks fitted to the Meteor which have not yet been fully analysed. They should prove interesting as a preliminary analysis indicates that the effect of the tanks on the static position error may be considerable at high Mach numbers.

A small amount of flight work is necessary to check the accuracy of trailing static measurements at high Mach numbers. Firstly, some dives at reduced engine power are required in order to verify the pressure lag correction, and secondly some high Mach number tests on a varying tow length arc required to find the disturbance from the aircraft that reaches the trailing static.

It is possible that the trailing static might prove to be invaluable in investigating the nature of position error at high Mach numbers. The results so far obtained on the Meteor are of considerable interest and it is felt that the trailing static should be fitted to an aircraft capable of transonic speeds should such an aircraft become available for this purpose. Such a test would also be useful in determining whether or not the head can be successfully flown in the transonic region.

The use of the instrument for routine position error measurement is not likely, because of the considerable time that may have to be devoted to obtaining a satisfactory installation in any aircraft. But as a means of fundamental position error investigation the trailing static may prove extremely useful. Its accuracy is very good provided that a calibration of the trailing static head can be obtained (a tunnel calibration will be required if the head is used at Mach numbers much higher than those reached on the Meteor), and also results can readily be obtained under 'g'.

It is also hoped to be able to investigate pitot error at high Mach numbers and lift coefficients, by replacing the trailing static head by a pitot one.

8.2 Possible limitations of use of the trailing static

It is difficult to estimate the maximum Mach number at which the trailing static can be towed satisfactorily. The head has been designed to have a high critical Mach number (probably about 0.9) and no towing trouble is envisaged below this speed. Above this there will inevitably be longitudinal trim changes on the head which must finally be in the sense to reduce the downward lift. Coupled with a possible increase in pipe drag this may impose a limit on the towing Mach number.

With the values of trailing static C_p so far employed, the measured trail angle (defined as the angle between the Meteor chord line and the line between the crutch and the trailing static) is about 20° at $M = 0.8$ and 30,000 ft. Furthermore, this angle appears to be increasing with increasing Mach number, which suggests a possible decrease in pipe drag. This fact is encouraging with regard to use of the trailing static at higher Mach numbers.

8.3 Use of the Meteor as a "calibrated datum"

The static pressure error of the Meteor having been calibrated under a variety of conditions, it is now possible to use this particular aircraft as a basis for high altitude 'aneroid' tests on other aircraft. The method consists of flying the test aircraft past the Meteor at approximately the same altitude, noting the altimeter readings of the two aircraft as they pass and measuring (by photographic means) the geometrical height between the two aircraft.

The results so far obtained by using this technique are encouraging. An accuracy of about ± 0.0075 in pressure coefficient at $M = 0.7$ and 35,000 ft altitude seems to be obtainable in level flight calibration, the limit being set by the accuracy of the altimeters.

9 Conclusions

(1) A trailing static head has been successfully used up to a Mach number equal to 0.84. Provided that the slight possibility of certain systematic errors being present can be excluded, then an accuracy of ± 0.0025 in Mach number can be obtained.

(ii) The variation in static position error of the Meteor installation with Mach number agrees fairly well with the value predicted by the Glauert law as far as $M = 0.75$, provided that C_L is small. Beyond this the true Mach number is higher than predicted (0.018 higher at $M = 0.843$).

At larger C_L 's the actual Mach number begins to be higher than the estimated value at about $M = 0.5$.

(iii) The flight value of the pressure calibration of the trailing static head agrees with the tunnel value to within $\pm 0.3\%$ of $\frac{1}{2}\rho v^2$. The original difference of $1\% \times \frac{1}{2}\rho v^2$ between flight and R.A.E. standard pressure calibrations was reduced to $0.3\% \times \frac{1}{2}\rho v^2$ when the flight calibration was compared with the R.A.E. long tube static head calibration. The flight calibration is the first absolute static head calibration that has been obtained since tests on the N.P.L. whirling arm in 1912.

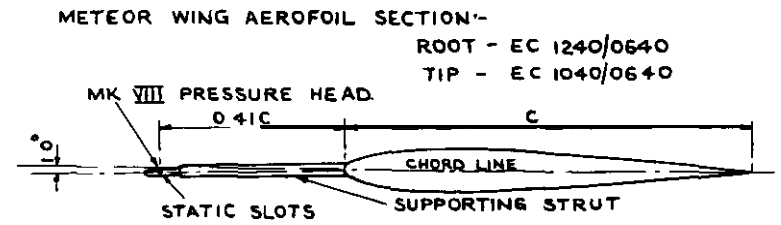
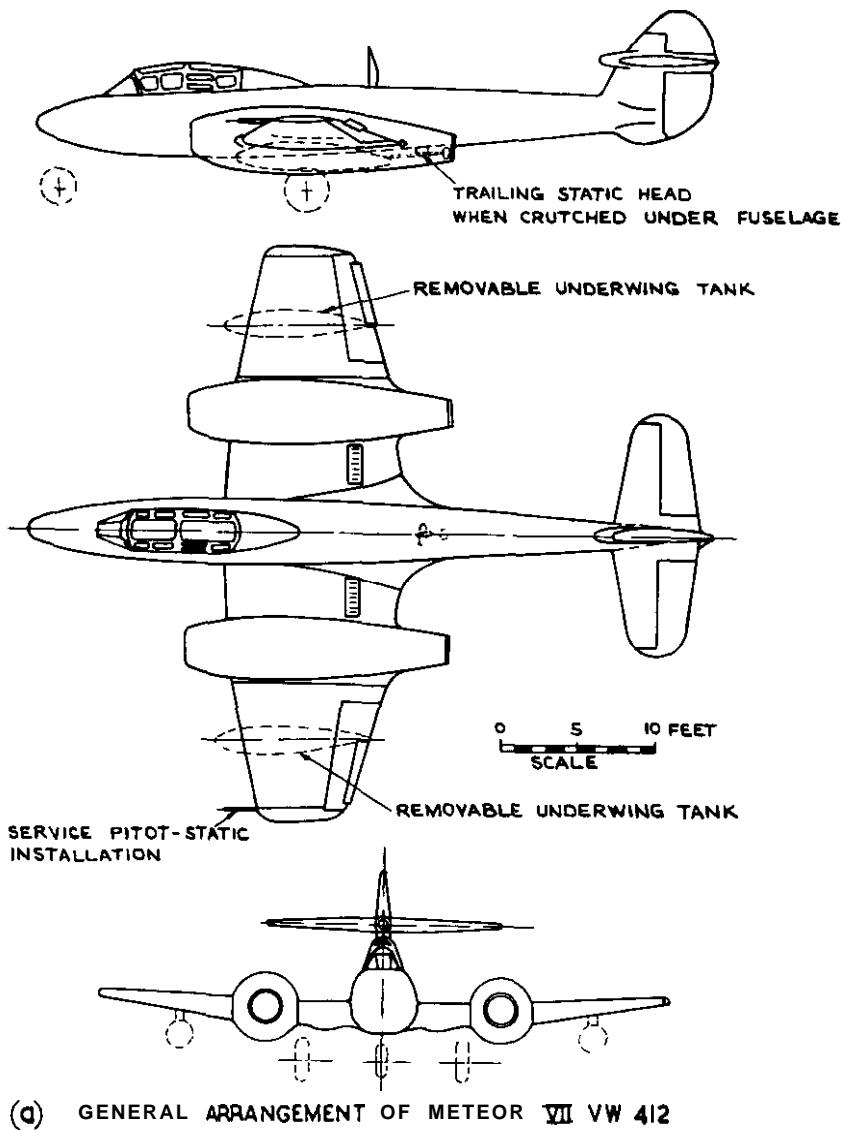
(iv) It is not known to what extent the trailing static head can be used in the transonic region. It is felt that should a suitable aircraft become available the head should be tried at transonic speeds, and if successful should be used for a fundamental investigation of position error at these Mach numbers.

REFERENCES

<u>No.</u>	<u>Author</u>	<u>Title, etc.</u>
1	Weaver	The calibration of Air Speed and Altimeter Systems. ARC 12,564 August 1949
2	Charnley and Fleming	Corrections applied to Air-speed Indicator and Altimeter Readings for Position error and Compressibility Effects. ARC 12,365 February 1949
3	Cameron	Note on the Effect of Position error on Compressibility correction ARC 5747 and 5748 May and September 1941
4	Lock, Knowles and Pearcey	The Effect of Compressibility on Static Heads R & M 2386 January 1943
5	Rogers and Berry	Tests on the Effect of Incidence on Some Pressure Heads at High Subsonic Speeds C.P. No. 41 July 1950
6	Huston	Accuracy of Airspeed Measurements and Flight Calibration Procedures N.A.C.A. Report No. 919 (1948)
7	Bramwell, Relf and Fage	On the determination on the whirling arm of the pressure velocity constant for a pitot (velocity head and static pressure) tube; and on the absolute measurement of velocity in aeronautical work. R & M 71 (December 1912)

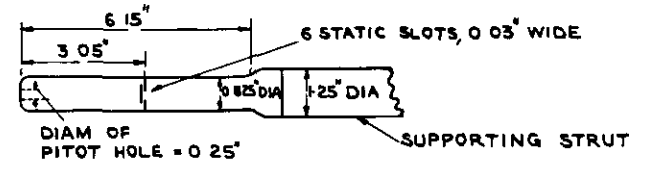
NOTATION

P_S	pressure recorded by aircraft static head
P_s	true static pressure in the free stream
P_T	pressure recorded by trailing static head
$\frac{1}{2}\rho V^2 = \frac{\gamma}{2} M^2 P_s$	dynamic head in free stream
$\Delta P_S = P_S - P_s$	static pressure error of aircraft static head
$\Delta P_T = P_T - P_s$	static pressure error of trailing head
$\Delta C_P = \frac{\Delta P_S}{\frac{1}{2}\rho V^2}$	static pressure error coefficient of aircraft static head
V_R	A.S.I. reading corrected only for Instrument error
M	free stream Mach number (assuming no correction to pitot)
M_1	indicated Mach number
$\Delta M = M_1 - M$	Mach number error
n	total normal acceleration of aircraft ('g' units)
CL	lift coefficient (relating either to aircraft or model)
$\gamma = 1.40$	ratio of specific heats for air



DETAILS OF SECTION AT PRESSURE HEAD

LOCAL CHORD (FT) (C)	5.75
MAX AEROFOIL THICKNESS AS FRACTION OF CHORD	10%
POSITION OF MAX THICKNESS AS FRACTION OF CHORD FROM LE	40%
CAMBER AS FRACTION OF CHORD	+0.6%
DISTANCE OF STATIC SLOTS AHEAD OF LE (FT) (0.41C)	2.35
INCLINATION OF AXIS OF PRESSURE HEAD RELATIVE TO CHORD LINE	1° NOSE DOWN
SPANWISE DISTANCE OF PRESSURE HEAD FROM WING TIP (FT)	0.75



(b) DETAILS OF MK VIII PRESSURE HEAD

FIG 1. a & b DETAILS OF AIRCRAFT & AIRSPEED INSTALLATION.

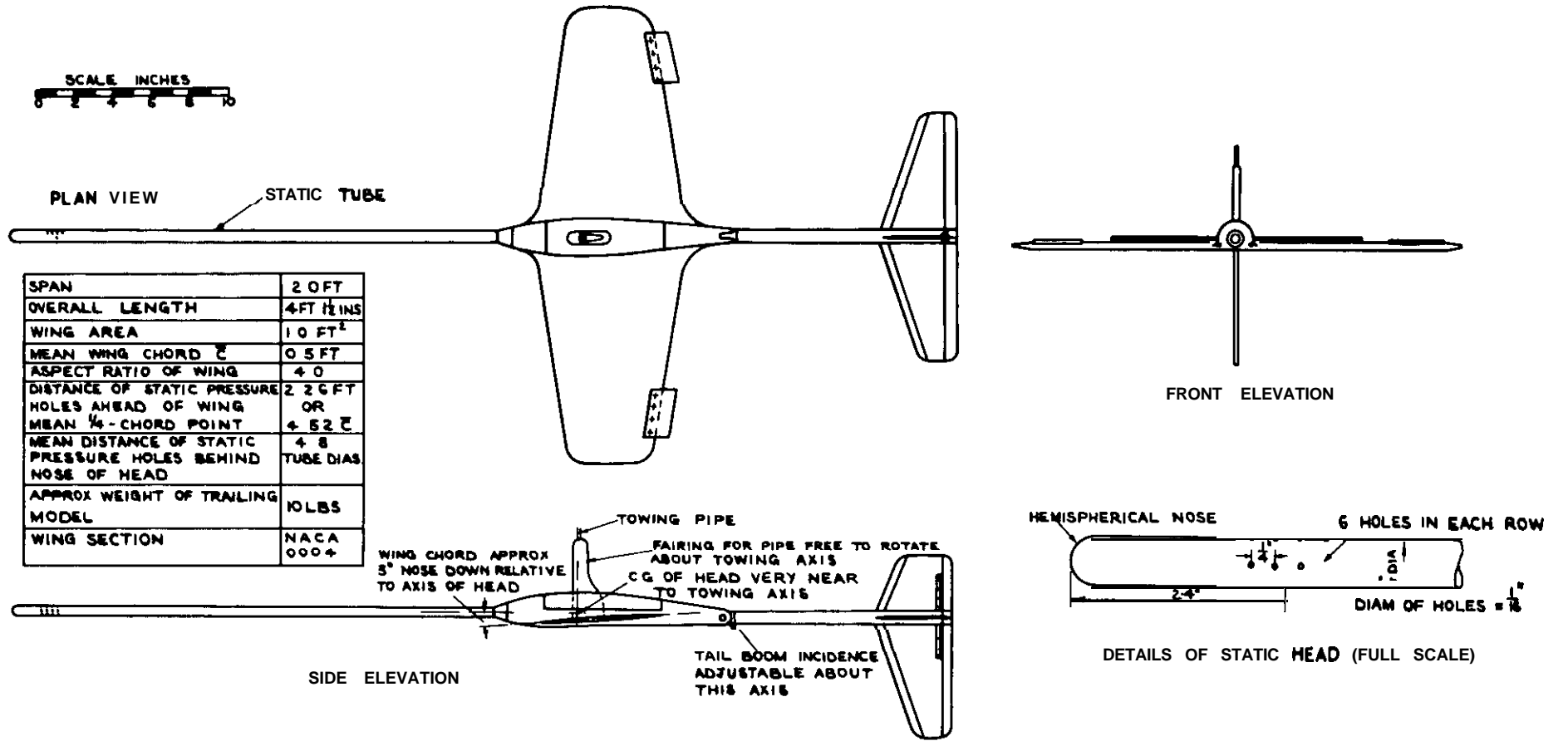


FIG.2. THE HIGH SPEED TRAILING STATIC HEAD

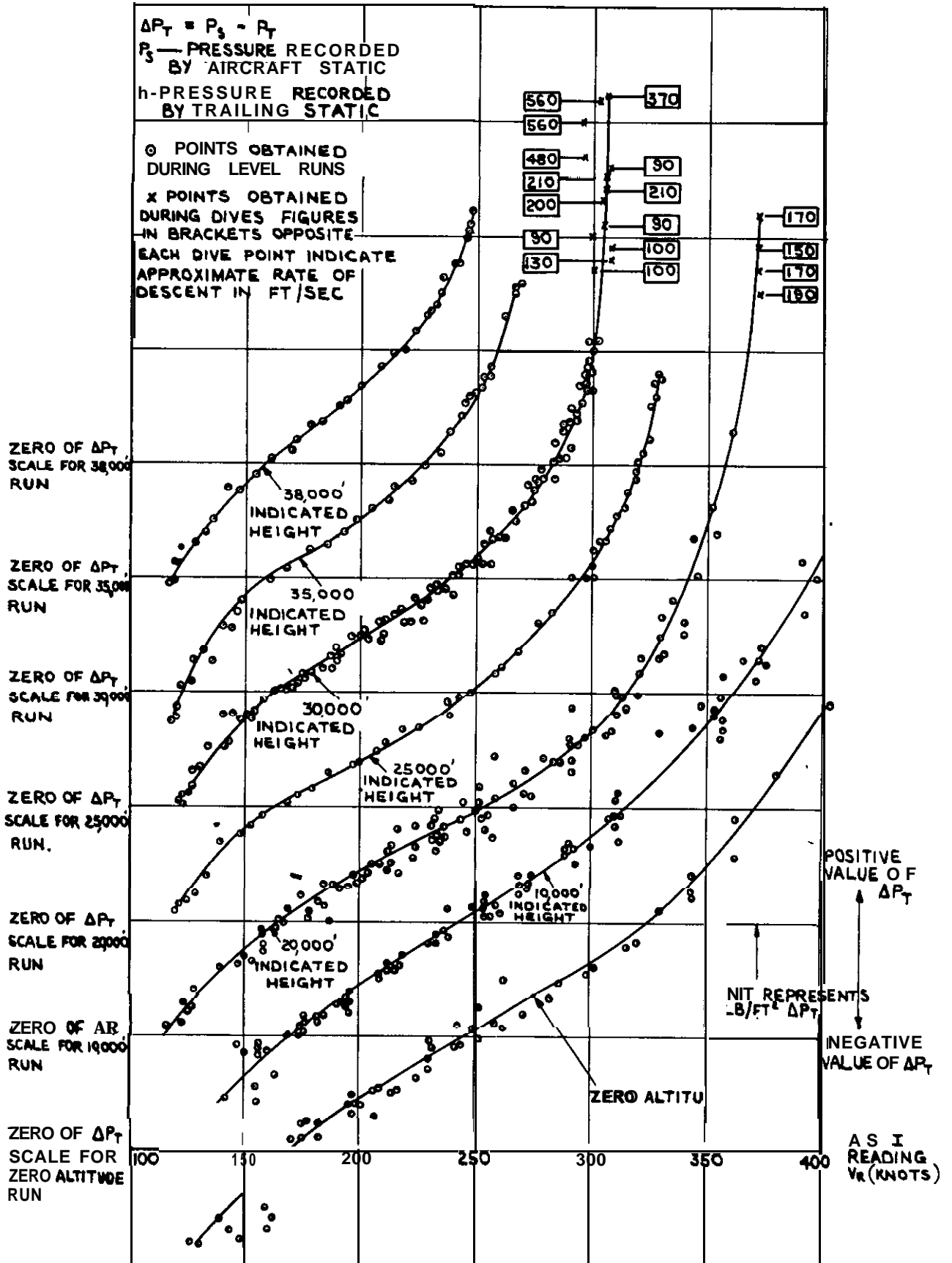


FIG. 3. APPARENT STATIC PRESSURE ERROR AS MEASURED BY TRAILING STATIC IN UNACCELERATED FLIGHT AT DIFFERENT ALTITUDES (NO UNDERWING TANKS.)

FIG4

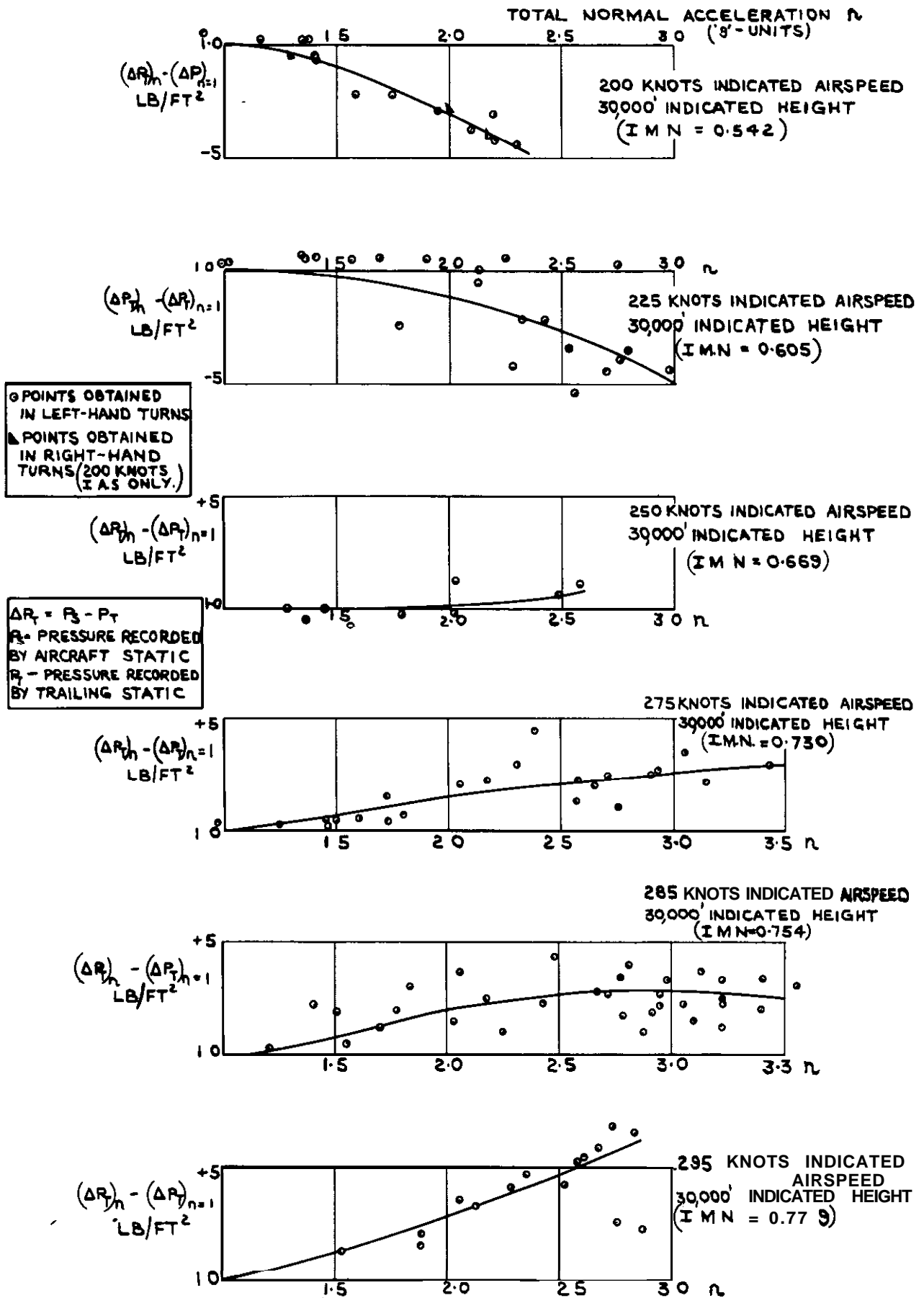


FIG. 4 EFFECT OF 'G' ON STATIC PRESSURE ERROR AT VARIOUS AIRSPEEDS - RESULTS OBTAINED BY TRAILING STATIC IN STEADY TURNS AT 30,000' INDICATED HEIGHT (NO UNDERWING TANKS.)

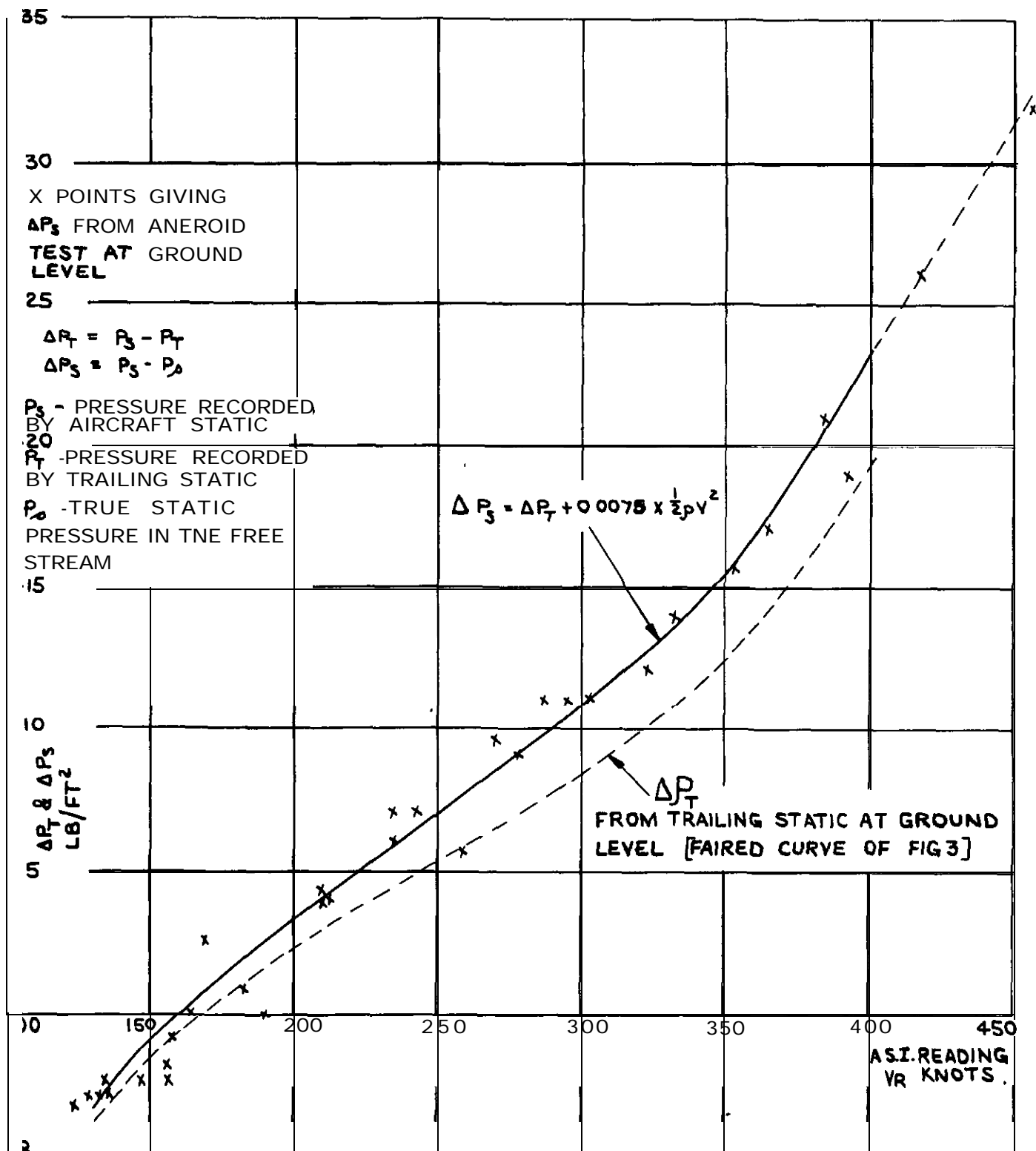


FIG. 5 (a) COMPARISON BETWEEN APPARENT AND TRUE STATIC POSITION ERRORS AT GROUND LEVEL. (NO UNDERWING TANKS)

FIG.5 b

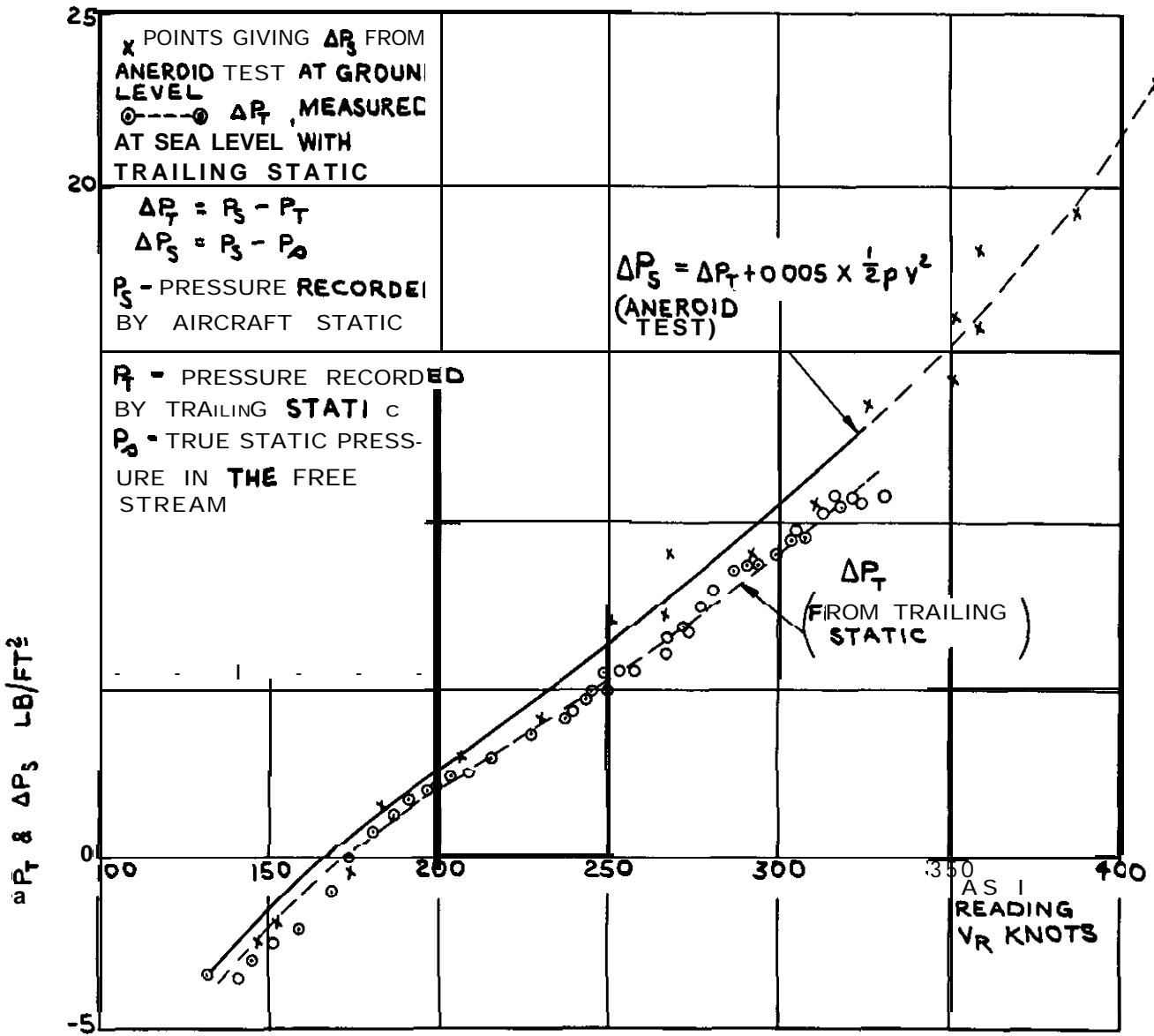


FIG.5 (b) COMPARISON BETWEEN APPARENT AND TRUE STATIC POSITION ERRORS AT GROUND LEVEL (WITH UNDERWING TANKS)

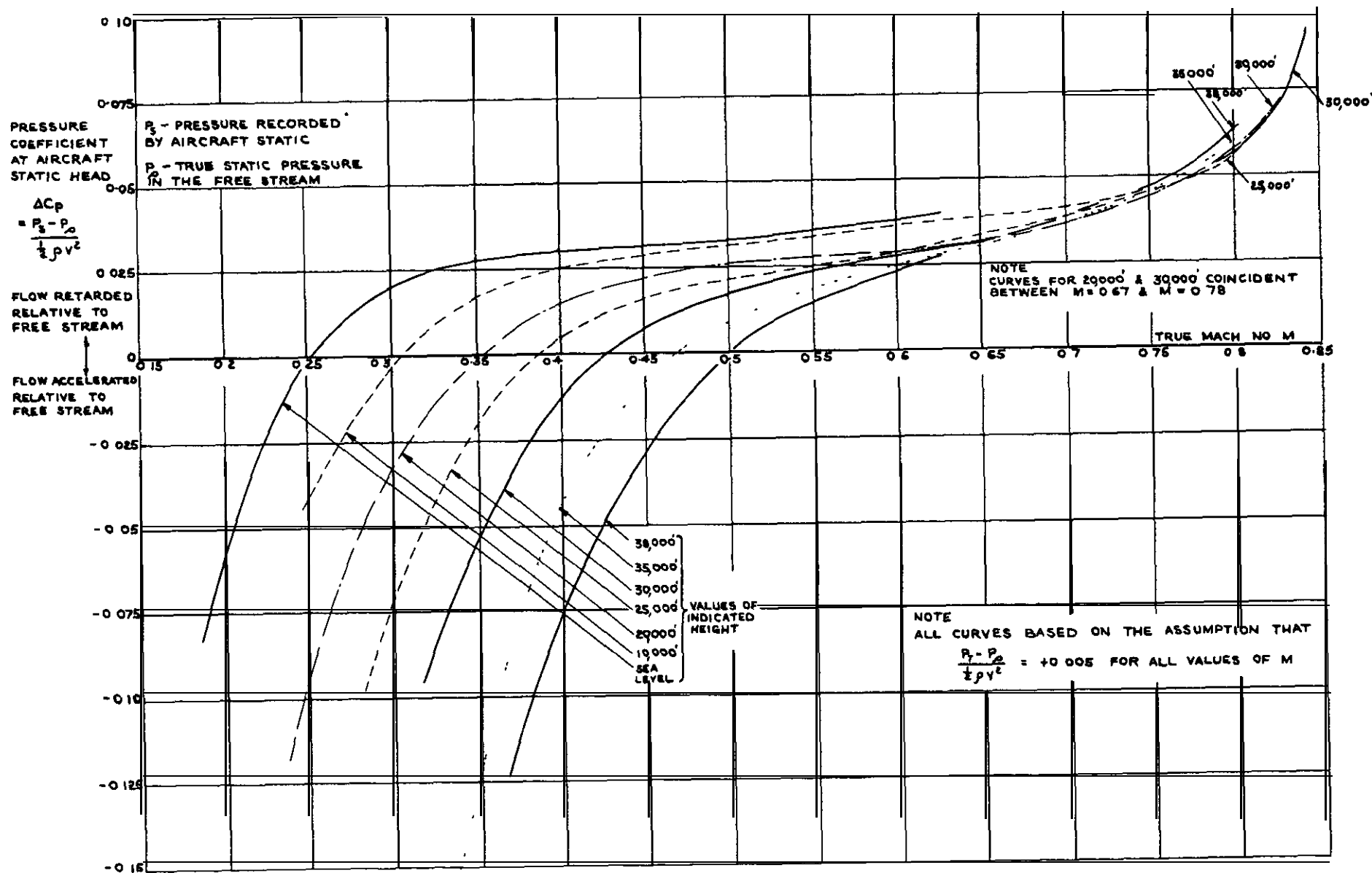


FIG.6 STATIC PRESSURE ERROR COEFFICIENT AS A FUNCTION OF MACH NUMBER FOR A SERIES OF ALTITUDES - UNACCELERATED FLIGHT (NO UNDERWING TANKS.)

FIG.7

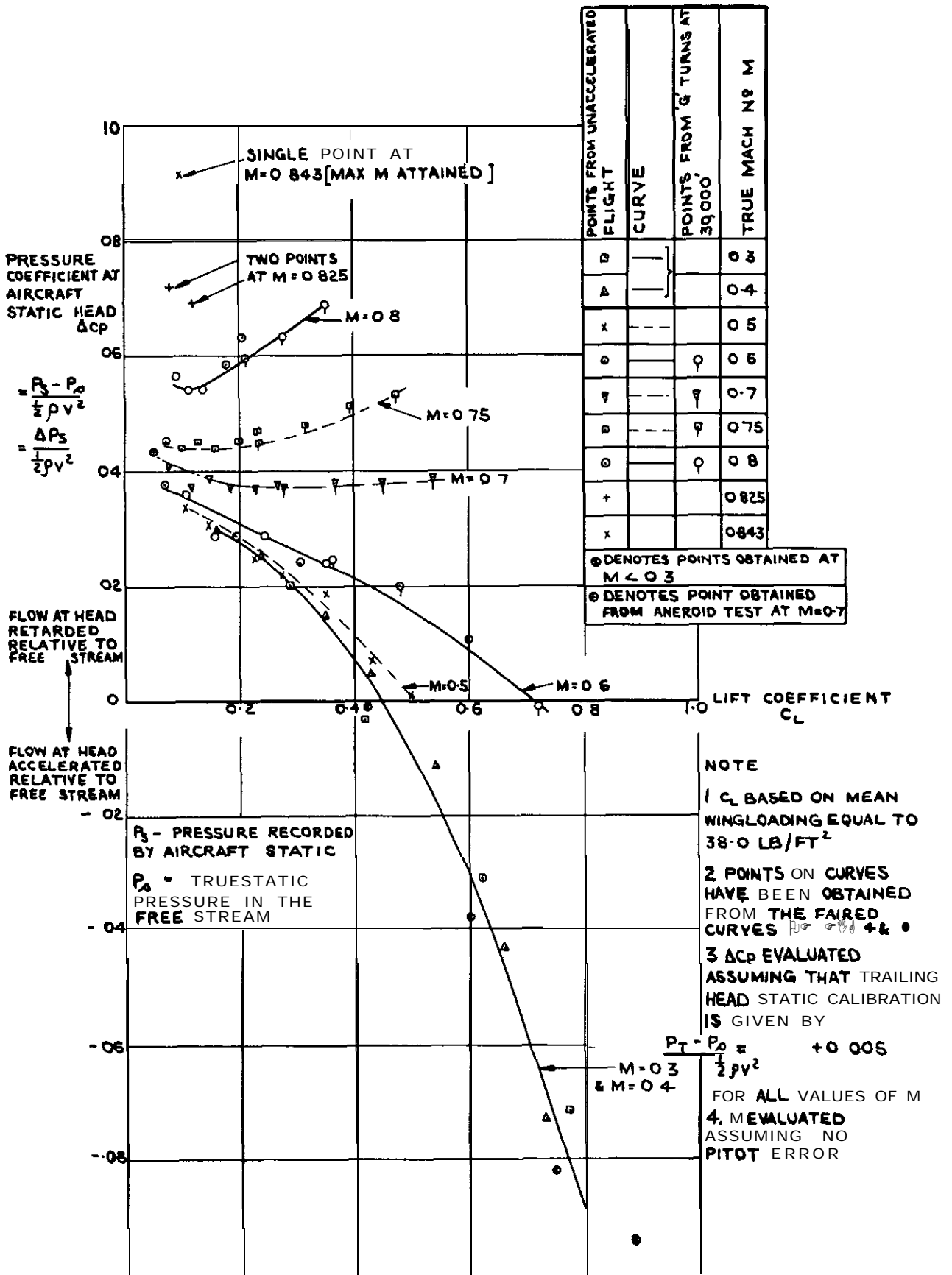


FIG.7 STATIC PRESSURE ERROR COEFFICIENT AS A FUNCTION OF LIFT COEFFICIENT FOR VARIOUS VALUES OF MACH NUMBER - UNACCELERATED FLIGHT AND 'G'-TURNS (NO UNDERWING TANKS)

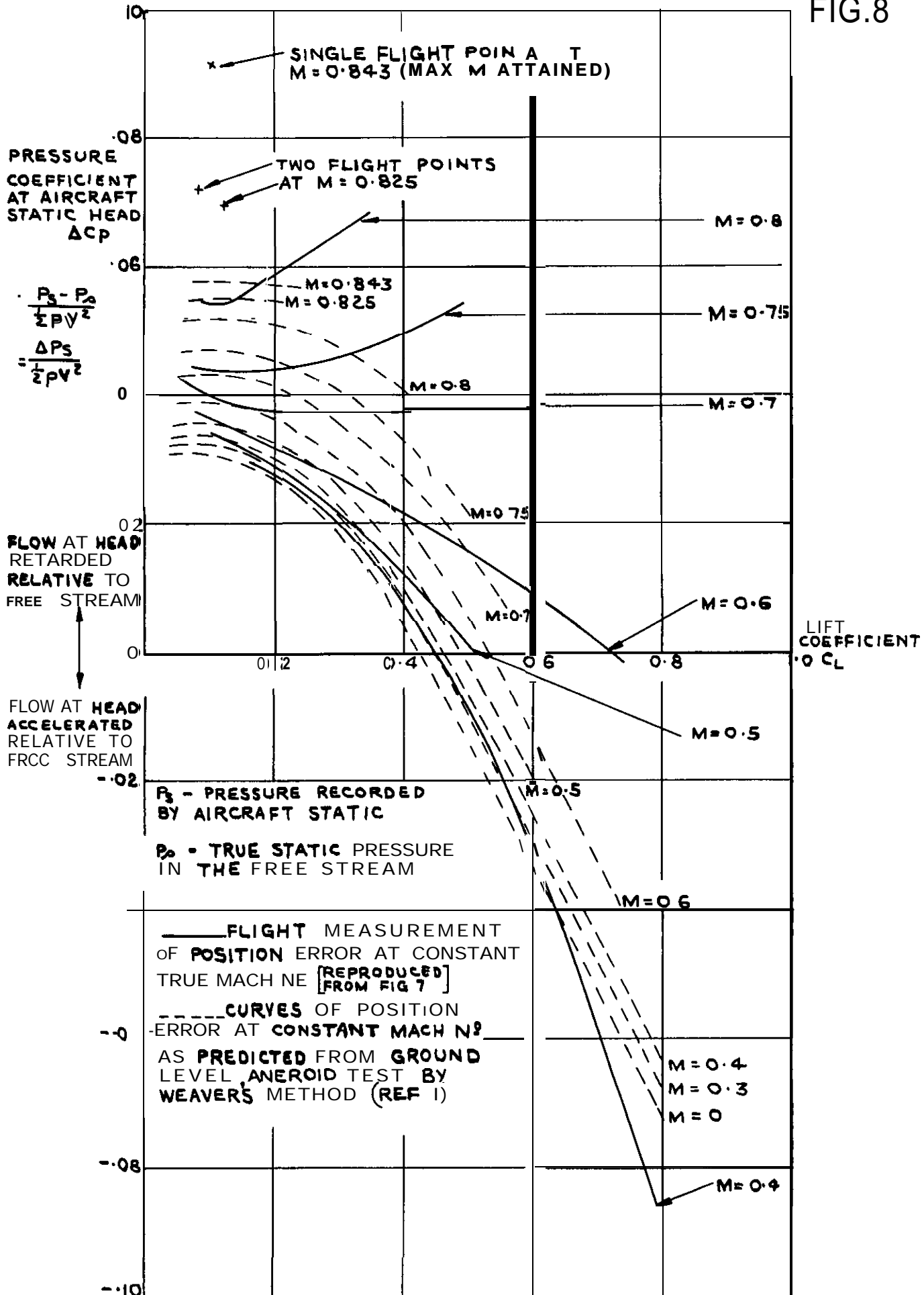


FIG. 8 COMPARISON BETWEEN FLIGHT VALUES OF STATIC ERROR & THOSE PREDICTED FROM GROUND LEVEL ANEROID TEST BY WEAVERS METHOD. (NO UNDERWING TANKS)

FIG. 9

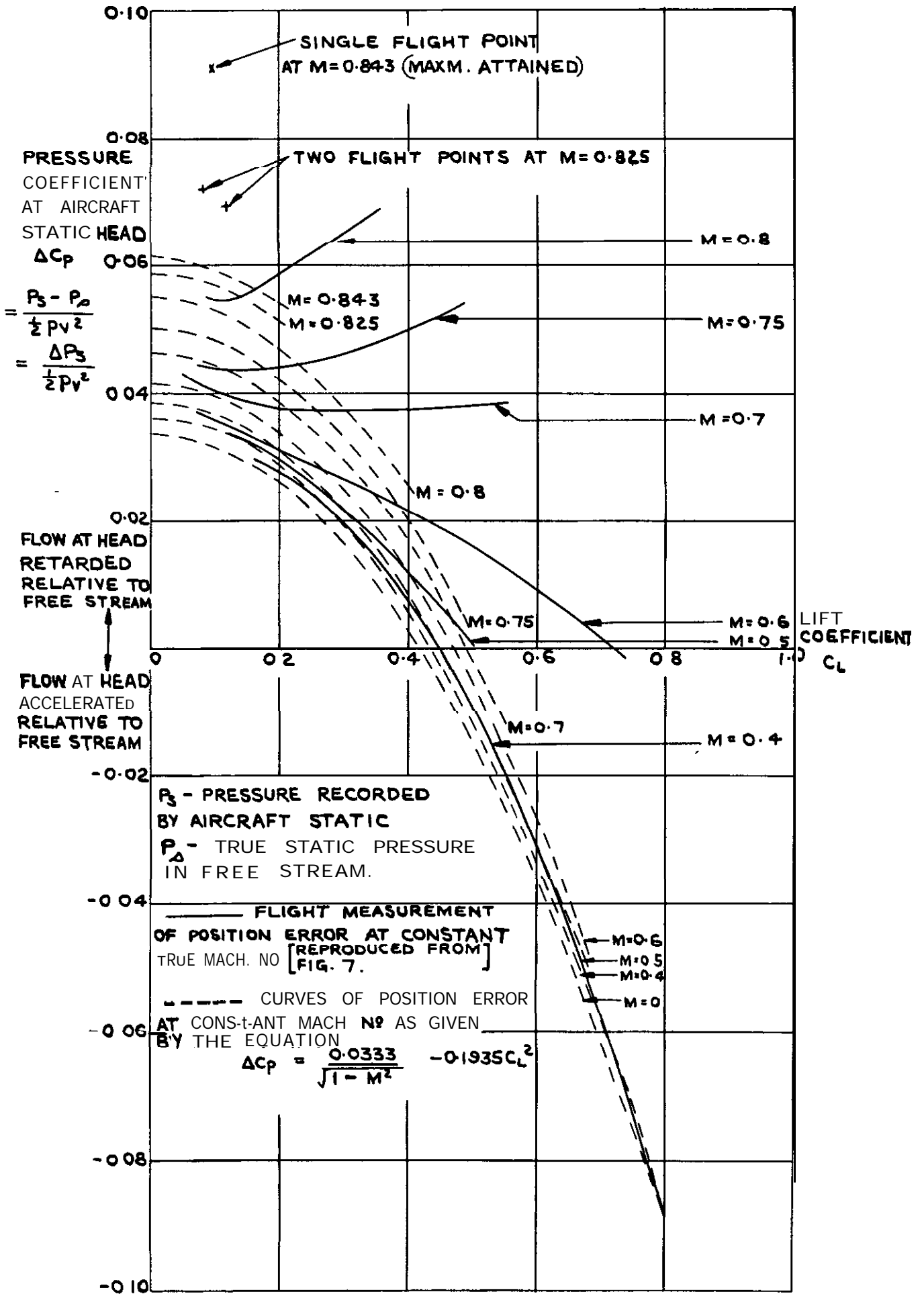


FIG.9 COMPARISON BETWEEN FLIGHT VALUES OF STATIC ERROR AND THOSE PREDICTED BY EQUATION OF THE FORM $\Delta C_p = \frac{\Delta C_{p0}}{\sqrt{1 - M^2}} - K C_L^2$

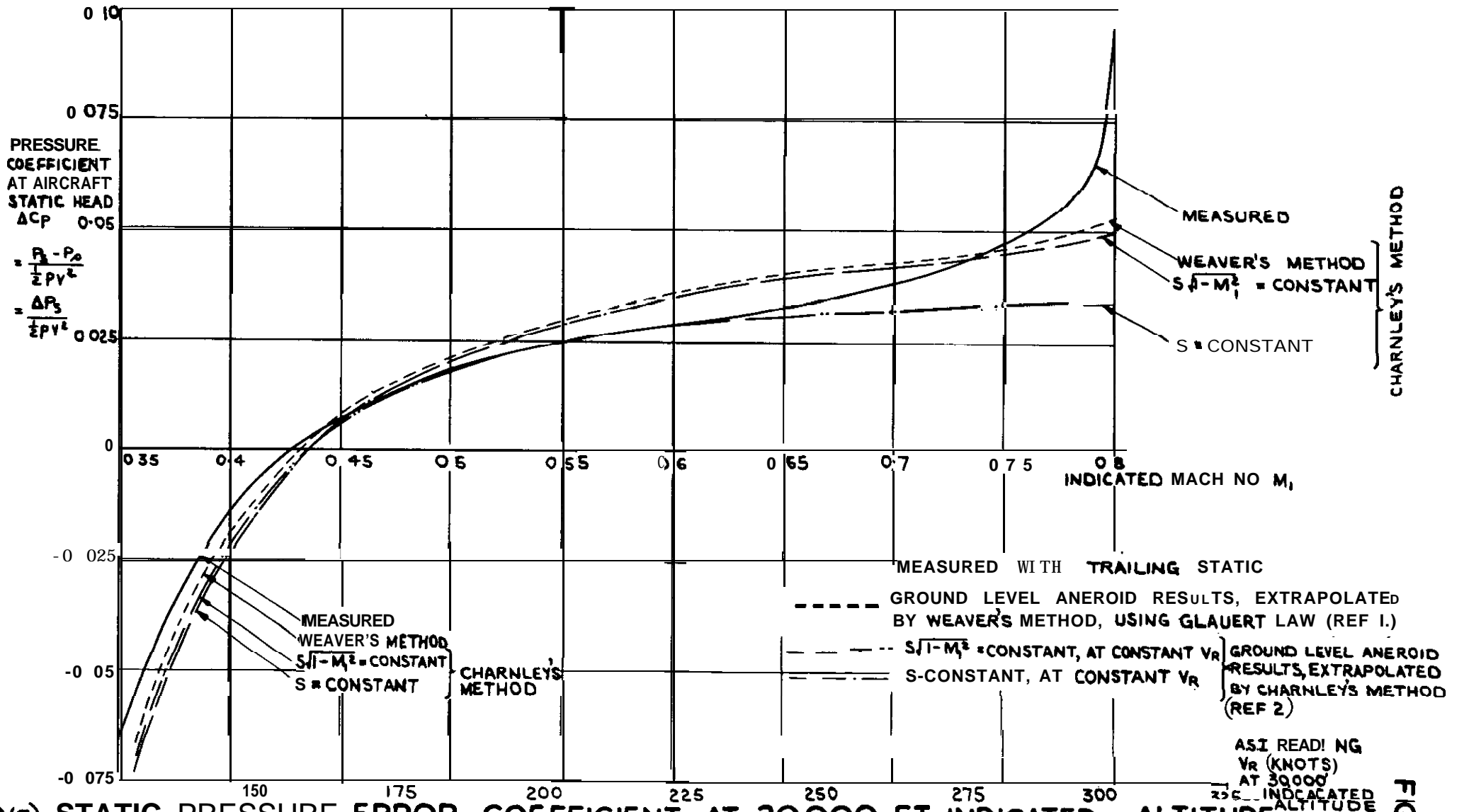


FIG 10(a) STATIC PRESSURE ERROR COEFFICIENT AT 30,000 FT. INDICATED ALTITUDE - COMPARISON BETWEEN MEASURED VALUES & THOSE FOUND FROM EXTRAPOLATION OF GROUND LEVEL RESULTS. (UNACCELERATED FLIGHT.)

FIG.10(a)

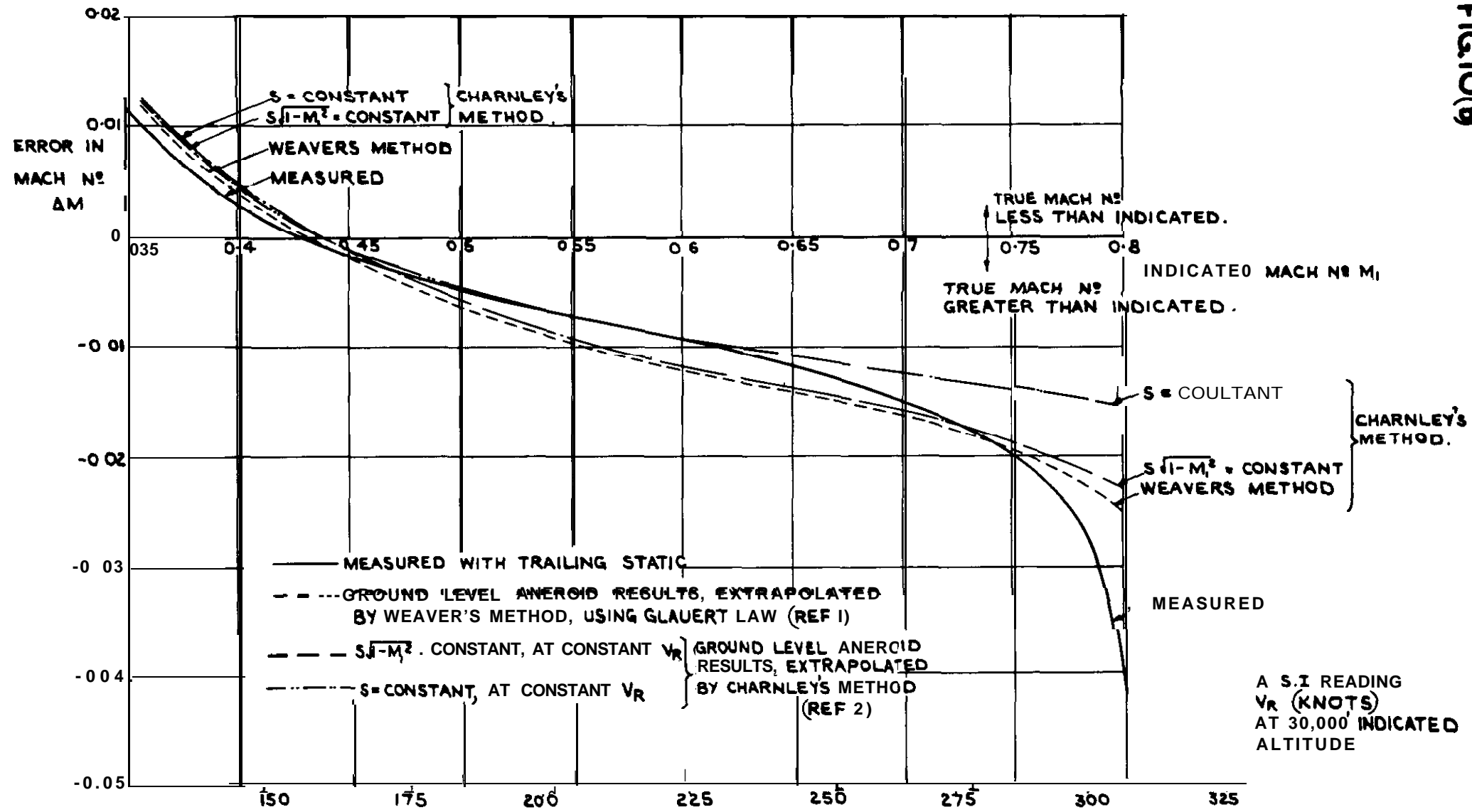
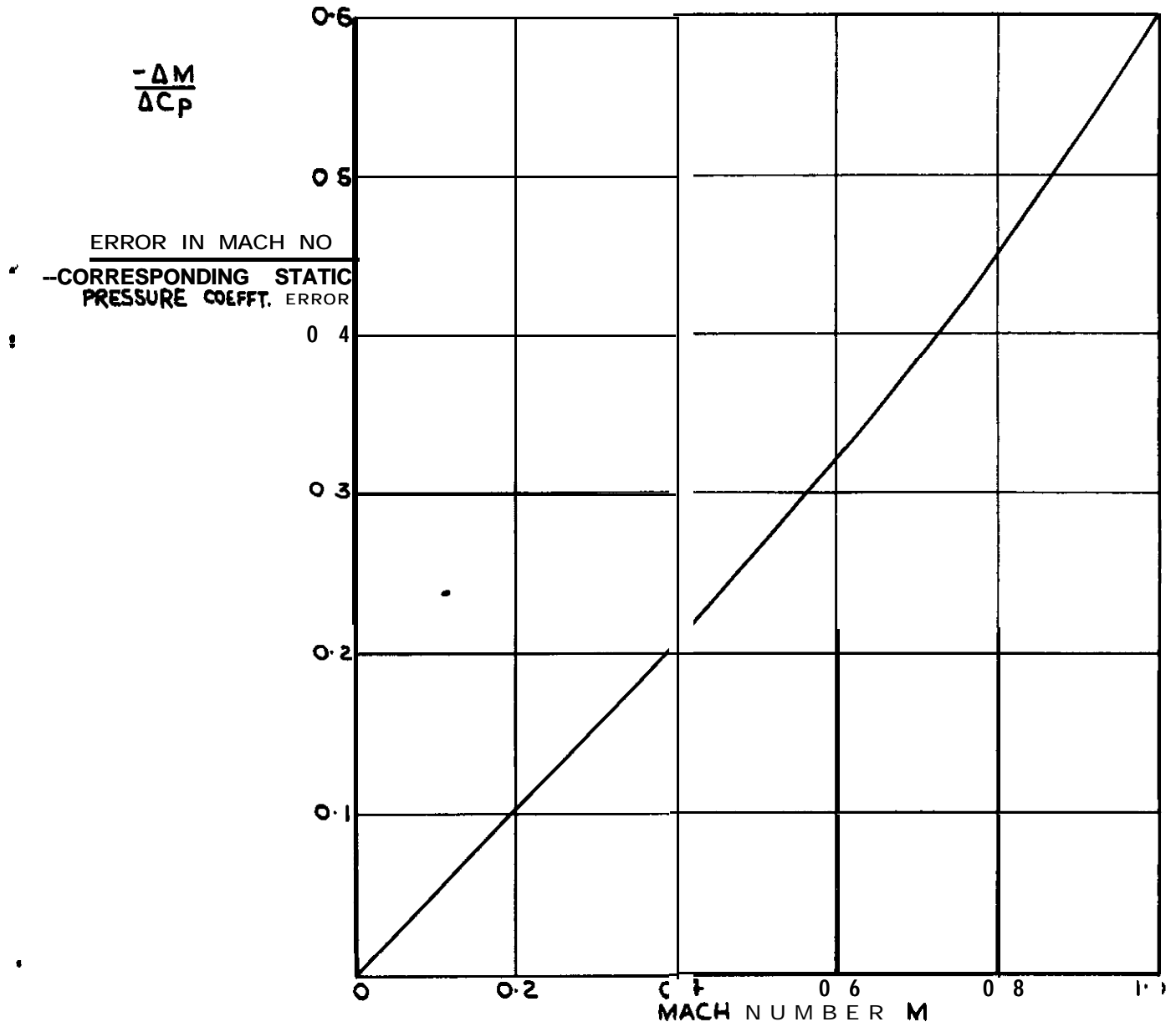


FIG. 10. b MACH NUMBER ERROR AT 30,000 FT. INDICATED ALTITUDE—COMPARISON BETWEEN MEASURED VALUES & THOSE FOUND FROM EXTRAPOLATION OF GROUND LEVEL RESULTS (UNACCELERATED FLIGHT.)



$$\frac{\Delta M}{\Delta C_p} = -\frac{M}{2} \left[1 + \frac{\gamma-1}{2} M^2 \right] \quad \text{[EQUATION 73]}$$

$$\gamma = 1.40$$

ΔM = ERROR IN MACH NUMBER

$$\Delta C_p = \frac{\Delta P_s}{\frac{1}{2} \rho V^2} = \text{STATIC PRESSURE ERROR, EXPRESSED IN COEFFICIENT FORM}$$

TOTAL HEAD PRESSURE ASSUMED TO BE MEASURED CORRECTLY.

FIG.1 I RELATION BETWEEN STATIC PRESSURE ERROR AND CORRESPONDING MACH NUMBER ERROR IN SUBSONIC FLOW (FIRST ORDER THEORY)

FLT. 88
30,000 ft.
346 m p h
IND.
M = .79

Indicated Airspeed = 301 Knots
Indicated Altitude = 30,000 ft.
True mach number = 0.815
Model lift coefficient = -0.28
'Braided' cable used (length 78 ft.)

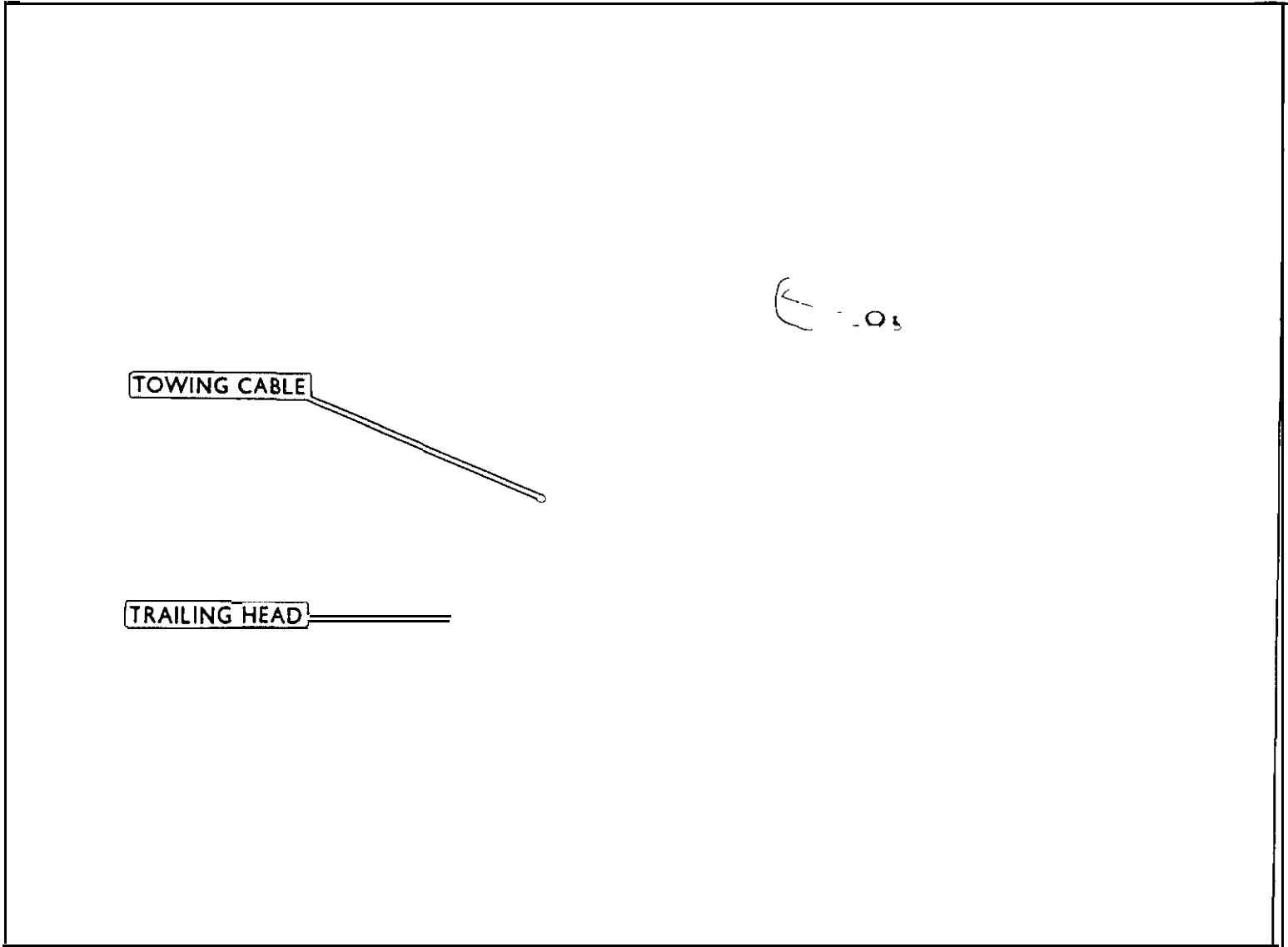


FIG.12. THE TRAILING STATIC HEAD BEING TOWED BEHIND METEOR

Crown Copyright Reserved

PUBLISHED BY HER MAJESTY'S STATIONERY OFFICE

To be purchased from

York House, Kingsway, LONDON, W C 2, 423 Oxford Street, LONDON, W 1
P O Box 569. LONDON, S E 1

13a Castle street, EDINBURGH, 2 1 St Andrew's Crescent, CARDIFF

39 King street, MANCHESTER, 2 Tower Lane. BRISTOL, 1

2 Edmund Street, BIRMINGHAM, 3 80 Chichester Street BELFAST

or from any Bookseller

1954

Price 3s. Od. net

PRINTED IN GREAT BRITAIN